Int. J. Heat Mass Transfer. Vol. 20, pp. 635–646. Pergamon Press 1977. Printed in Great Britain

BUBBLE FORMATION AND HEAT TRANSFER DURING DISPERSION OF SUPERHEATED STEAM IN SATURATED WATER—I

BUBBLE SIZE AND BUBBLE DETACHMENT AT SINGLE ORIFICES

HANS SCHMIDT
Institut für Reaktorbauelemente, Gesellschaft für Kernforschung, 75-Karlsruhe, Germany

(*Received* 17 *March* 1976 *and in revised form* 12 *August* 1976)

Abstract—Despite the high practical importance of heat and mass transfer between fluid phases the relevant data are not well known due to the multitude of parameters affecting this phenomenon. This paper deals with part of this extended problem by restriction on the events taking place during bubble formation at single orifices.

Subject of this paper is the experimental investigation of bubble formation and detachment from single submerged orifices at high system pressures and temperatures. In Part II the corresponding heat transfer is investigated.

The experiments are carried out in the steam–water system. The superheated steam is injected through 1.5, 2 and 3 mm diameter orifices from a 5 cm³ antechamber into demineralized saturated water. The steam flow rate is varied in the range of 2–20 g/min, the maximum pressure is 212 at. The examinated steam temperature differences related to the corresponding boiling temperatures are 100, 150 and 200 K.

The experimental observations are interpreted by means of dimensional analysis. The following results are obtained: Relations are pointed out between the bubble shape as well as the formation frequency and the physical parameters of the system.

The relevant effect on transition from steady-state bubble formation (single bubble formation) to unsteady-state bubble formation (coalescence of the bubble during detachment) is found to be a problem of eigenoscillation of the bubble.

NOMENCLATURE

b, Laplace constant;
c, c_p, specific heat;
d, orifice diameter;
f, frequency;
g, acceleration of gravity;
h, height of the column of water;
$\dot{m}$, mass flow rate;
n, eigen frequency;
p, pressure;
r, radius;
V, volume,
O, surface;
T, temperature;
Re, $= \dfrac{\dot{m}}{d \cdot \eta_0}$, Reynolds number;
We, $= \dfrac{\dot{m}^2}{d^3 \sigma \rho_0}$, Weber number;
Fr, $= \dfrac{\dot{m}^2}{g d^5 \rho_0^2}$, Froude number;
Eu, $= \dfrac{p \rho_0 d^4}{\dot{m}^2}$, Euler number;
Ec, $= \dfrac{\dot{m}^2}{d^4 c_p \rho_0 (T_0 - T')}$, Eckert number;
Str, $= \left(\dfrac{d}{g}\right)^{1/2} \cdot f$, Strouhal number.

Greek symbols

η, viscosity;
Δ, difference;
ν, kinematic viscosity;
ρ, density;
σ, coefficient of boundary surface tension;
ω, angular frequency.

Indices

Ab, detachment;
O, orifice;
R, numerical value;
V, antechamber;
1, 2, steam, water;
$'$, $''$, saturation state of water/steam phase.

1. INTRODUCTION

IN MANY technical applications gas or steam is fed into liquid either to cause a chemical reaction or to give rise to heat and/or material transfer [1, 2]. In most cases the gas or steam is introduced into the liquid via horizontal nozzle plates and passes through a multitude of cylindrical bores. During escape from such a bore (orifice) the formation of bubbles at the orifice is observed under certain conditions. The size of such bubbles and the frequency of their formation, which are the subjects of this part of the work, are of considerable interest in many practical applications; they exert a substantial influence on heat and mass transfer between the gas and liquid phases.

During bubble growth at an orifice the pressure in the interior of the bubble is subjected to changes, partly because the curvature of the phase boundary continuously undergoes variations and partly because the hydrostatic pressure of the effective liquid column decreases through the ascent of the phase boundary.

Restricting the consideration to these two pressure conditions, we obtain the type of static bubble formation which can be determined theoretically. The liquid movements caused by bubble growth and detachment as well as the flow through the orifice of the gas entering the bubble are neglected. The equilibrium of forces existing at such interface is described by the capillary theory, e.g. [3]. Under the conditions of aeration encountered in technical applications the static mode of consideration is mostly inadequate while dynamics gains a substantial influence. The movement of the gas–liquid interface is influenced by the mass flow into the bubble, by the inertia of the liquid to be displaced, by the frictional drags existing at the phase boundary, and possibly by heat and mass exchange [4–8].

The bubbles detach periodically from the orifice. The mass flow rate through the orifice is thereby interrupted for a short interval. Consequently, the pulsation of the flow is coupled with the mechanism of bubble formation which again is influenced by the gas supply system [9]. So far, the influence of the physical properties of the gas (viscosity and density) on bubble formation and detachment have largely been left unconsidered. However, when the system pressure is varied, the pressure-dependent difference of physical properties between the gas and the liquid becomes more significant, which calls for the inclusion of the gas or steam properties.

This part of the work will deal with the experimental investigation of bubble formation and bubble detachment in liquid aeration through cylindrical single orifices at high system pressure and temperature.

2. EXPERIMENTAL SETUP

The experimental setup is represented in Fig. 1.

A metering piston pump circulates the water against the pressure in the test vessel. The water is vaporized in a capillary tube with direct resistance heating and the steam is superheated to the desired temperature. By pressure equalizing reservoirs and high flow resistance of the capillaries a pulsation-free steady-state mass flow is generated into the antechamber. From this heated antechamber the steam flows through a cylindrical orifice into the pressure vessel filled with water at saturation temperature. Through lateral windows made of synthetic sapphire and provided at the test vessel the process of bubble formation and detachment is recorded with a high-speed camera. The equipment has been designed for a pressure of 230 at and a temperature of 673 K. The tests are performed while the following parameters are varied:

The system pressure p (<40; 40, 80, 120, >160 at), the mass flow through the orifice $\dot{m}$, the orifice diameter d (1.5; 2; 3 mm), the steam superheat $T_v - T'$ (100, 150, 200 K) and the height of the column of water h. The flow of superheated steam is varied in such a way that a zone is covered beginning with the regular formation of different bubbles, the so-called steady-state bubble formation, via the zone of bubble coalescence in the vicinity of the orifice, the so-called unsteady-state bubble formation, and ending by bubble chains, the so-called turbulent aeration. The volume of the antechamber $V = 5\,\text{cm}^3$ and the height of the orifice $h_0 = 4\,\text{mm}$ are kept constant.

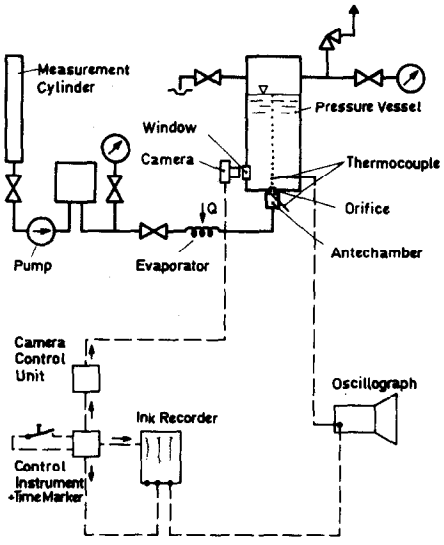

FIG. 1. Experimental set-up (schematic).

3. EXPERIMENTAL RESULTS

The physical properties are varied by change of the system pressure and superheated steam temperature while the variation of the mass flow causes a change in kinetic energies. Together with the orifice diameter this variation influences the time depending development of the bubble growth, the geometric shape of the bubbles, and the process of detachment.

The influence of the mass flow rate is shown in Fig. 2, the different pictures of which characterize 3 zones of dynamic aeration.

The picture on the top marks the steady-state zone in which single bubbles are observed with specific bubble volumes and formation frequencies attributable to the respective mass flow through the orifice. The central picture represents the non-steady-state zone in which the bubbles coalesce in pairs or in groups at increased mass flow rates. The volume of detachment and the frequencies of formation are subjected to variations. At high mass flow rates the zone of gas jets is reached in the bottom picture. The bubbles are no longer formed at the edge of the orifice but at the crest of a gas jet flowing into the liquid.

The influence of the system pressure on the size and shape of the bubbles formed is shown in Fig. 3. The system pressure has been varied in five steps from 12 to 212 at. The orifice geometry, the mass flow, and the superheat temperature remain constant. At a pressure of 12 at large volume bubbles are formed. When the system pressure is increased to 80 and 150 at, respectively, the volumes of the bubbles become smaller. At 180 at the contours of the bubbles are no longer axially symmetric. A further increase of the pressure to 212 at entails the destruction of the bubble contours and a diffuse steam jet is observed.

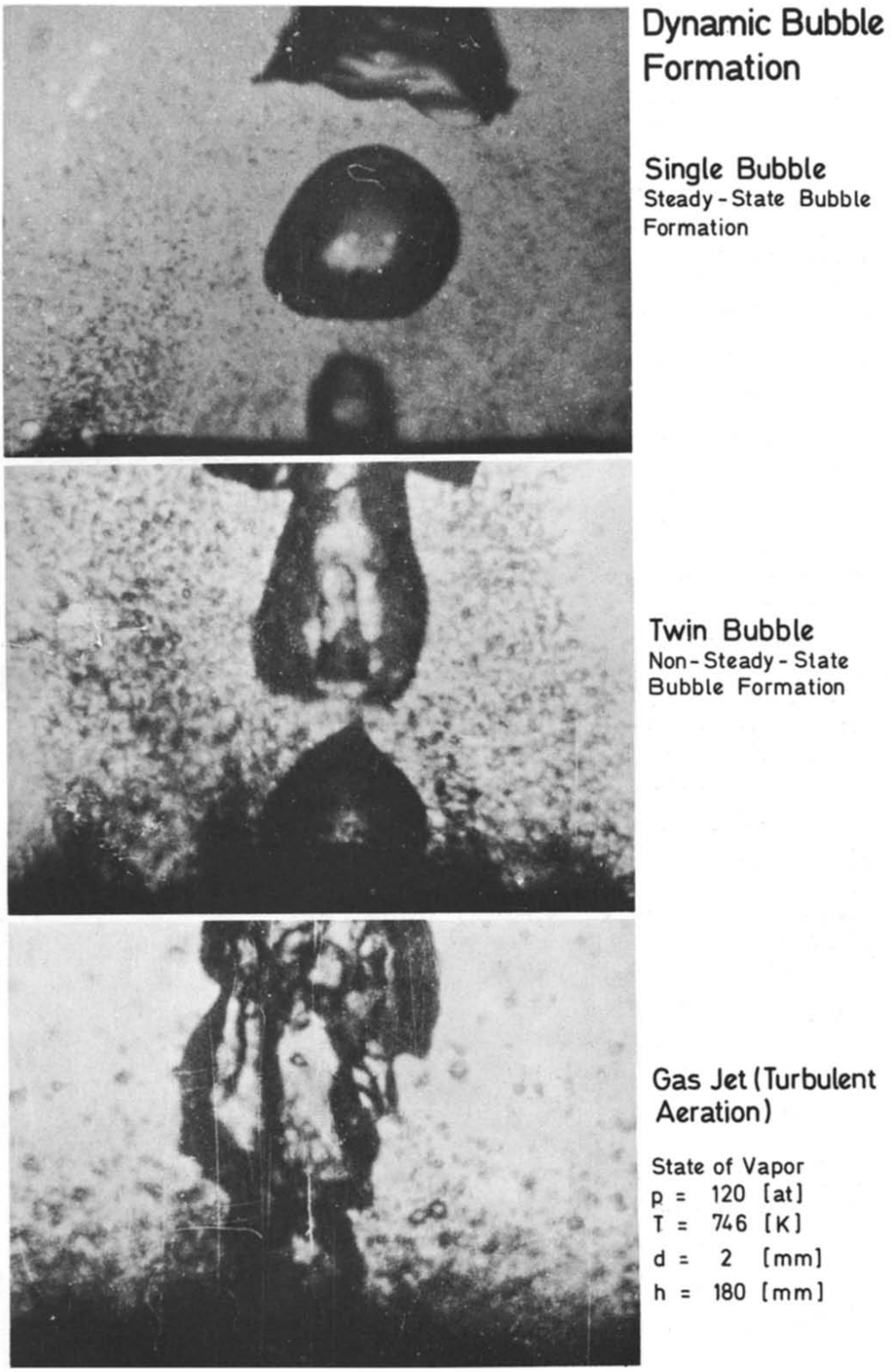

FIG. 2. Aeration (steady-state, non-steady-state, turbulent).

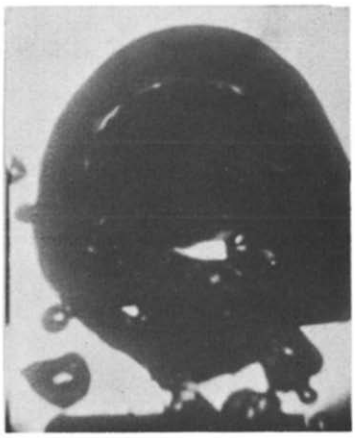

p = 12 at

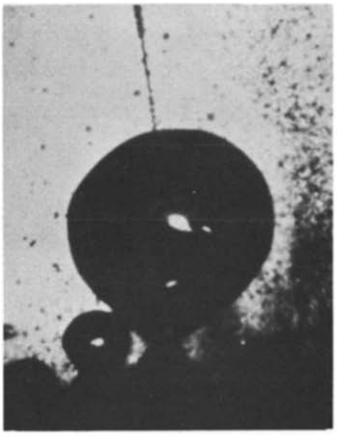

p = 80 at

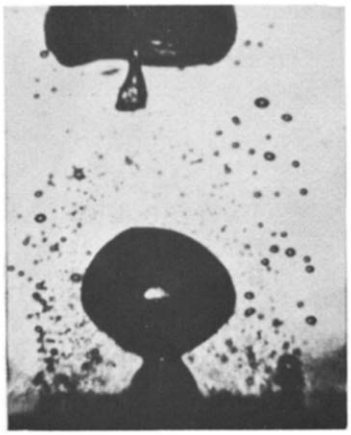

p = 150 [at]

p = 180 [at]
Steam Jet

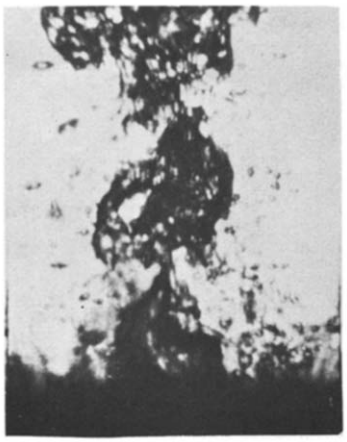

p = 212 [at]
Incipient Destruction of
Interface

Superheated Steam - Saturated Water
Orifice Dia.= Const. = 3mm
Mass Flow = Const. = 5g / min
Steam Superheat = Const. = 150K
Enlargement = 5x

FIG. 3. Types of aeration (dependent on system pressure).

The essential results of this test series consist in the decrease in bubble size with increasing system pressure and the change of the bubble shape at high system pressures.

For an orifice diameter of 3 mm in Fig. 4 the volumes of the bubbles at the time of detachment are plotted versus the mass flow. The volumes were calculated from the high-speed pictures assuming axially symmetric bubbles. The parameters are the system pressures 40, 80 and 120 at, and the superheated live steam of 100, 150 and 200 K associated with the respective pressures.

Two essential conclusions can be drawn from the diagram:

(i) The detachment volume of the bubbles increases with increasing mass flow.

(ii) The detachment volume decreases with increasing system pressure.

Starting from the balance of forces of a quasi-static bubble, i.e. if the dynamics of the steam and water phases remain unconsidered, the adhesion of the interface at the edge of the orifice ($\sigma\pi d$) and the buoyancy of the bubble ($Vg\,\Delta\rho$) at the time of bubble detachment are in equilibrium. The quasi-static mode of consideration assumes slow movements, i.e. long periods of bubble formation. Thus, the simplifying assumption that the steam in the bubble is cooled to nearly saturation temperature at the time of detachment may be regarded as valid (cf. Part II of this work).

The detachment volume is given by:

$$V = \frac{\sigma\pi d}{g(\rho' - \rho'')} = \pi d b^2 \qquad (1)$$

The expression $\sigma/g(\rho' - \rho'') = b^2$ is in units of an area. It represents the square of the so-called Laplace constant.

For the 3 mm dia. orifice a bubble volume $V = 32\,\text{mm}^3$ is calculated for $p = 40$ at, while for $p = 80$ at, $V = 22\,\text{mm}^3$ and for $p = 120$ at, $V = 15\,\text{mm}^3$ are calculated. These values have been plotted on the ordinate for $\dot{m} = 0$. With increasing system pressure the difference in densities $\rho' - \rho''$ becomes smaller; this means a decrease in buoyancy. At the same time, the decrease in the interface tension coefficient with increasing pressure leads to a drop of the adhesion. Since the interface tension coefficient decreases to a stronger degree in these pressure zones as compared to the difference in densities, the static equilibrium volumes becomes smaller with increasing system pressure.

The considerable deviation of the bubble sizes in such a way from that determined experimentally under the influence of mass flow shows that a supplement of the static mode of consideration by a dynamic one is necessary.

During bubble growth the phase boundary is displaced. The bubble must do work to displace the water. This requires an additional pressure in the bubble in order to displace the water. The amount of pressure increases with increasing rate of growth at the phase boundary, i.e. with increasing mass flow through the orifice and with decreasing system pressure. If the water displaced by the bubble is accelerated, the additional pressure present in the bubble and thus in the antechamber is reduced which leads to an increase in the flow of live steam in the bubble. The force due to inertia of the accelerated water causes a suction effect on the bubble and thus an additional feeding so that with growing mass flow rate and decreasing system pressure a much greater bubble volume can be observed than has been predicted by a static mode of consideration. Beginning with a system pressure of 120 at also the static mode of consideration yields quite useful information about the detachment volumes according to Fig. 4. At high system pressure smaller bubble volumes are formed with decreasing frequency of formation (Fig. 6). By the considerable rise in steam density less kinetic energy is supplied to the system, the phase boundary is advanced at a slower rate and via a shorter path in the water. The influence of displacement work decreases which means that the difference of bubble size remains small between the static and dynamic modes of consideration.

If the superheat temperature is increased at constant mass flow rates $\dot{m}$ and constant system pressure p, this

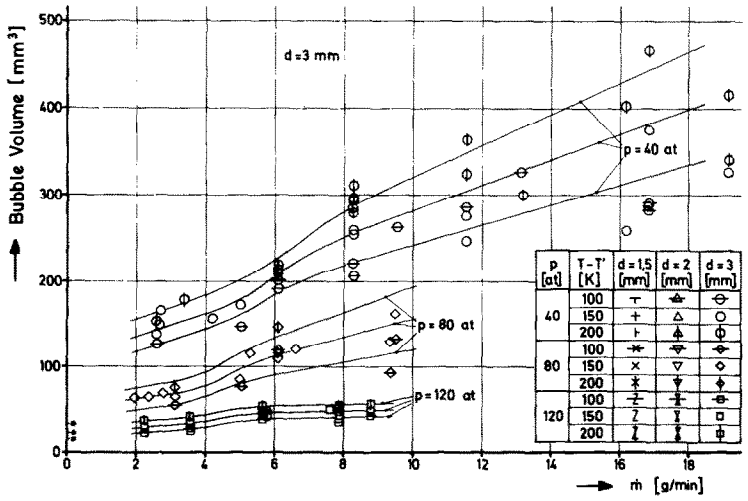

FIG. 4. Volume of detaching bubbles, orifice dia. 3 mm.

results in more displacement work by decrease of the steam density, implying the formation of larger bubbles during the same period of formation (Fig. 6). Here, the same tendency is observed as with respect to the decrease in system pressure discussed before.

The influence of the orifice size on the detachment volumes is shown in Fig. 5 and in Fig. 4. In Fig. 5 the bubble detachment volumes generated at cylindric

Besides a reduction in the detachment volumes following from a decrease of the orifice diameter a constriction of the bubble formation zones is observed. The decrease in bubble size is compensated by an increase in bubble sequence (Fig. 6). This means that the bubbles succeed one another with narrow spacing; the zone of mutual influencing during the process of detachment is displaced towards low mass flow rates.

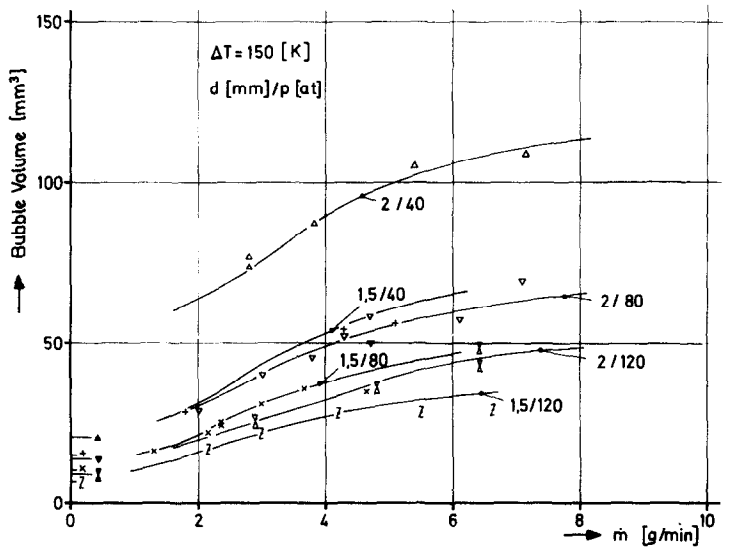

FIG. 5. Volume of detaching bubbles, orifice dia. 1.5 and 2 mm.

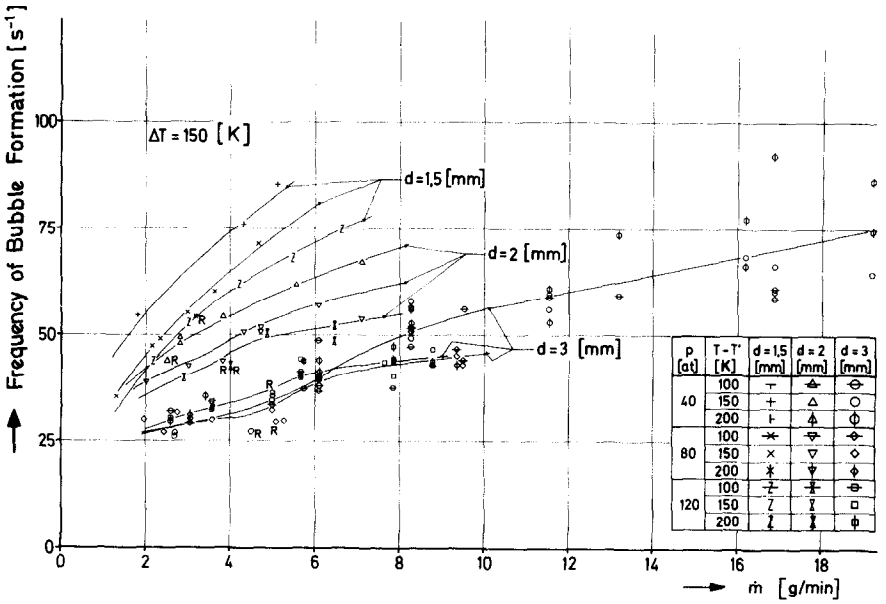

FIG. 6. Frequency of bubble formation.

orifices of 1.5 and 2.0 mm diameter have been plotted vs the mass flow. The diagram shows the system pressure as a further parameter. The superheating of steam is 150 K at all points of measurement. The statements made with respect to Fig. 4 are correspondingly applicable to that figure. It appears that a reduction of the orifice diameter leads to smaller bubbles because the adhesion decreases at the edge of the orifice.

For small orifices ($d = 1.5$ mm dia.) the frequency of bubble formation increases most according to Fig. 6. According to Fig. 5 this orifice has the lowest increase in detachment volumes with increasing mass flow. Generally, it can be observed that the gradient of formation frequency becomes smaller at high mass flow rates prior to attainment of turbulent aeration. A similar tendency of a frequency which is nearly constant over a defined

small range is also observed prior to transition from steady-state to non-steady-state bubble formation. With the 2 mm dia. orifice this range occurs at a mass flow of about 3 g/min, with a 3 mm dia. orifice at around 4 g/min. In this zone the increasing mass flow into the bubble is accommodated by greater bubble growth, i.e. by larger bubbles. The condition of non-steady-state aeration is attained with a more intensive increase in the average frequency of formation.

4. EVALUATION

Evaluating the measurements the determination of the area of the bubble surface can be regarded as a significant prerequisite of the further calculations, e.g. of heat and mass transfer. The bubble surface depends on the same parameters as the bubble volume. It proves to be difficult to determine quantitatively the effect of the dynamic forces acting at the phase boundary, which are caused by steam flowing into the bubble as well as by the water surrounding it. Both unsteady-state processes, steam and water dynamics, are coupled one to the other and exert an influence on the bubble formation. The tendencies as shown by the measuring results and the high-speed pictures allow to read the qualitative effect of the different limiting quantities. By the method of the π-theorem [10] the physical dimensionalized limiting qualities are obtained as dimensionless parameter groups, which can be interpreted as ratios of forces, energies and geometries (cf. Part II of this work).

According to Fig. 7 an appropriate combination of these characteristics allows to represent the functional relationship as a straight line. The resulting relation for the surfaces of detaching bubbles is given by equation (2).

$$Q = 1.913 \cdot 10^{-3} d^2 \left[\frac{Fr}{Re^2 \cdot We^2} \cdot \left(\frac{Re}{(Eu \cdot Ec)^{1/2}} \right)^{5.35} \right]^{1/3}. \quad (2)$$

The characterizing geometric variable in that expression is the diameter d of the orifice. Also the inertia, capillary, and buoyancy forces exert an influence on the bubble size. The product $(Eu \cdot Ec)$ is independent of the mass flow and of the orifice diameter and changes in the range experimentally considered only a little bit. Together with the other characteristics mainly the differences in steam superheating are fitted in this product. Equation (2) is an expression of the experimental results in the dynamic range of bubble formation with the following parameters:

system pressure	$p = 40, 80, 120$ at
Orifice diameter	$d = 1.5, 2, 3$ mm
steam superheating	$t = 100, 150, 200$ K.

The deviations of the calculated values from the experimental results are less than 20%. At the system pressure $p = 120$ at the deviations attain about 30% for the 1.5 and 3 mm dia. orifice.

Figure 8 shows the combination of the respective characteristics used to establish the functional relationship between the bubble formation frequency and the parameters of the system. The plot of the expression

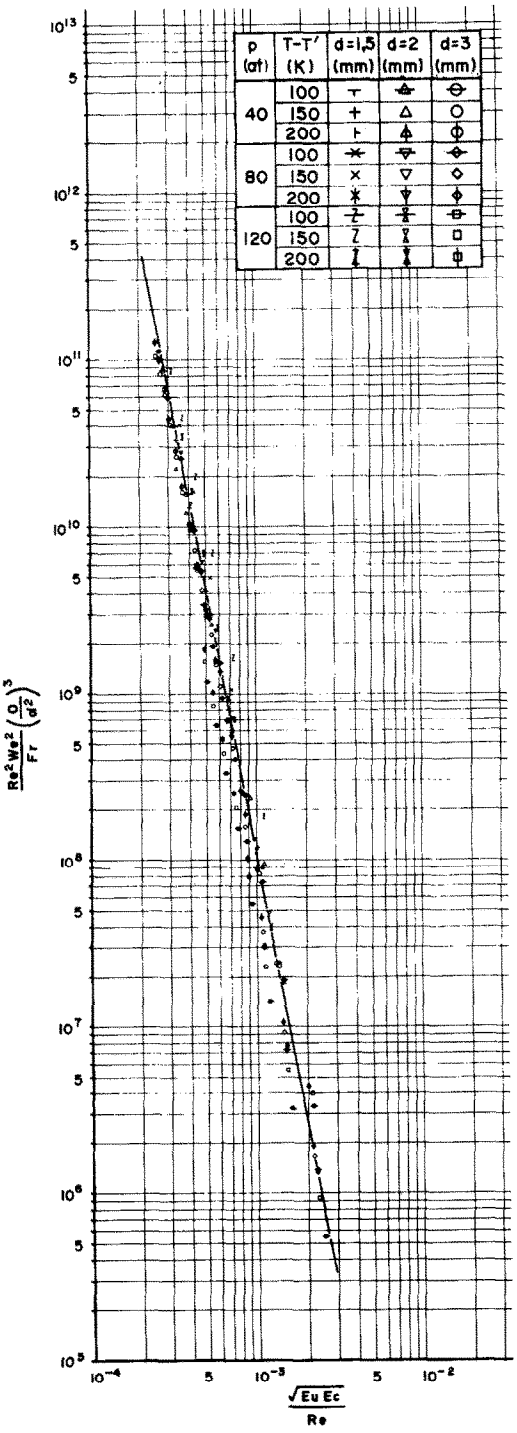

FIG. 7. Ratio of characteristics for representation of the dimensionless surface O/d^2.

$f \cdot (d/g)^{1/2}$ vs the Reynolds number is linear in the double logarithmic scale and thus the relation for the frequency of bubble formation at single orifices is given by equation (3):

$$f = 3.08 \cdot 10^{-2} (g/d)^{1/2} \cdot Re^{0.426}. \quad (3)$$

$f \cdot (d/g)^{1/2}$ must be interpreted as a Strouhal number characterizing unsteady-state flow. The evaluation of the high-speed films does not yield a dependence of the frequency of formation on the superheat temperature.

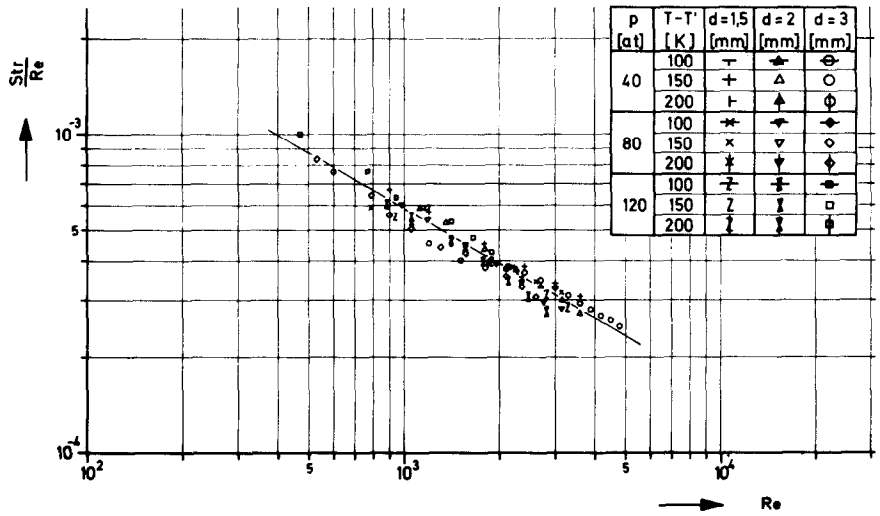

FIG. 8. Dimensionless frequency of formation.

Therefore, the Reynolds number has been established on the basis of the saturated steam viscosity. The deviation of the frequencies measured from the frequencies obtained from relation (3) is less than about 10%.

Slightly larger deviations around the transition point from steady-state to non-steady-state bubble formation will be indicated more accurately.

Taking into account additional test points not considered so far, the expressions obtained by dimensional analysis and empirical correlations seem to be applicable to provide information about the bubble surface and the frequency of formation in a pressure range extending from near atmospheric pressure to very high system pressure ($p = 160$ at).

As shown in Fig. 9 the bubble of a specific size detached from the orifice influences the formation of the following bubble. The latter bubble does not take the typical shape of a bubble but grows upwards rather quickly due to elongation and after a short period of formation it penetrates with a smaller volume into the preceding large bubble pushed inwards at its bottom side through detachment so as to become concave and coalesces with this bubble. This process is repeated. The reason for that periodic change can be explained by types of eigenoscillations. The general case of oscillation of a spheroid influenced by surface tension forces can be given by the Lamb formula of eigenoscillations [11, 12] in equation (4).

$$\omega^2 = n(n+1)(n-1)(n+2)\frac{\sigma}{[(n+1)\rho_1 + n\rho_2]r^3}. \quad (4)$$

A quantitative statement is obtained by the following steps. Two observations can be made from the high-speed film, the frequency of formation and the volume of detachment. Assuming spherical steam bubbles and using the detachment volume and the physical properties obtained from the operating data the frequencies of eigenoscillations are calculated according to the Lamb equation for three numbers ($n = 2, 3, 4$).

Figure 11 shows the difference between the measured frequency of formation and the calculated frequency of eigenoscillations.

If the differences of frequencies become zero, the frequency of bubble formation agrees with the eigenfrequency of the bubble. It can be seen from the high-speed pictures that the zero passage of the harmonic $n = 2$ and $n = 4$ does not exert an influence on the bubble formation. However, for the bubble oscillating in the third harmonic, the zero passage coincides with the onset of twin bubble formation. The excitation to make eigenoscillations comes from the bubble deformed by the process of detachment, which corresponds in shape to the third harmonic. The coincidence of the frequency of the formation and the frequency of the eigenmode causes an additional overshoot beyond the condition of equilibrium of the phase boundary and so gives rise to the process represented in Fig. 9.

Obviously, application of the Lamb formula primarily valid for the static case is only possible by the fact that at the much contracted bubble and in the absence of a gas feed through the orifice the phase boundary changes at such a low rate under the influence of the varying hydrostatic pressure due to the onset of upwards and water movements that a quasi-steady-state case of consideration becomes possible.

In the following paragraphs the frequencies of the oscillation mode of the third order are calculated for the transition point and compared with the measured frequency of formation. The bubble surfaces determined experimentally as well as the physical properties corresponding to the test parameters are used for the calculation. Equation (4) is transformed by means of the relation $\omega = 2\pi f$. The physical properties are substituted by the characteristics of the similarity mechanics.

This gives the dimensionless frequency f^x.

$$f^x = \frac{60}{(\sqrt{\pi})\left(1+\frac{3}{4}\frac{\rho'}{\rho}\gamma^{3/2}\right)}\cdot\frac{Fr}{We} \quad (5)$$

$$f^x = \frac{d}{g}f^2; \quad \frac{Fr}{We} = \frac{\sigma}{\rho g d^2}; \quad \gamma = \frac{O}{d^2}.$$

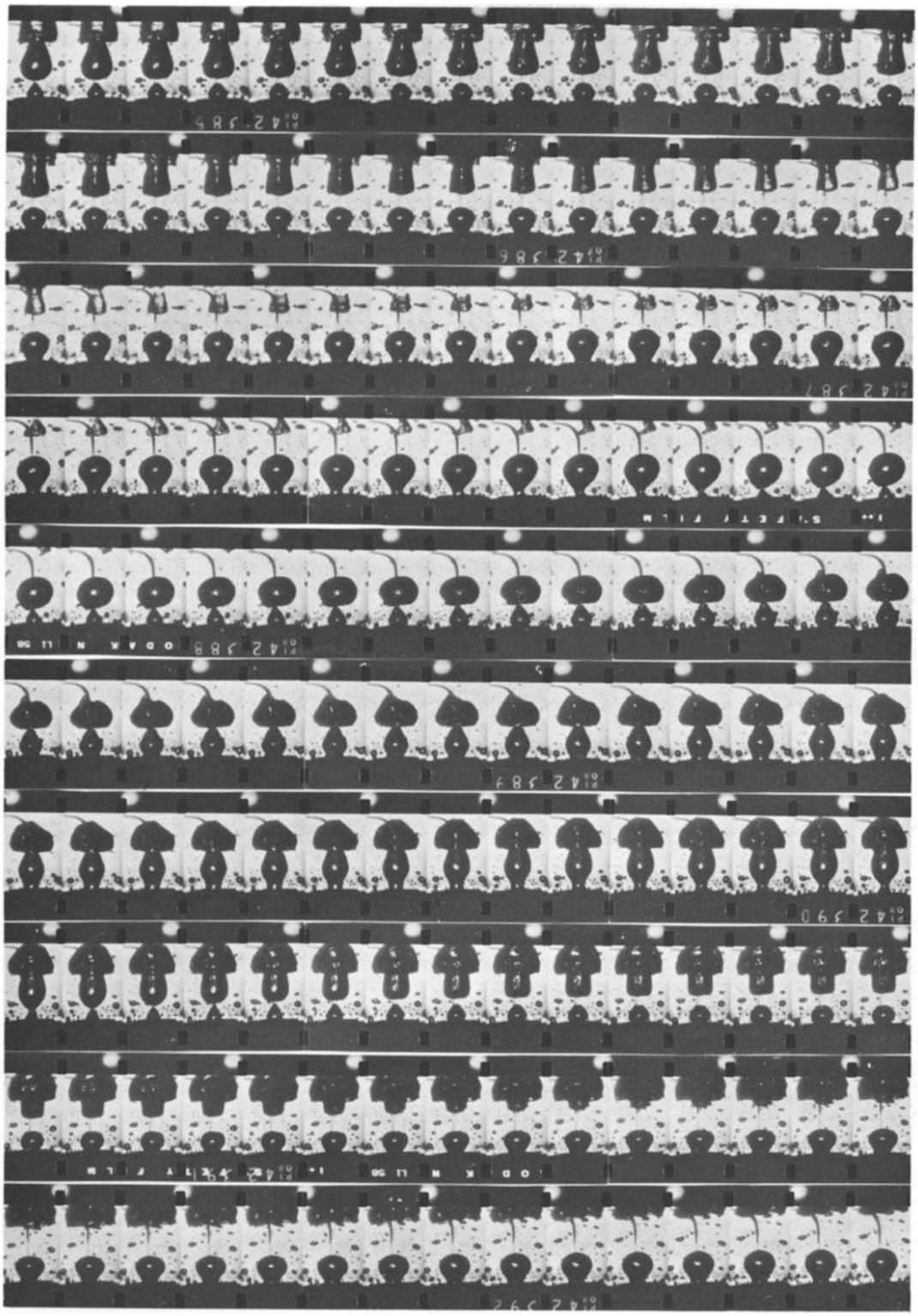

FIG. 9. Twin bubble formation.

The static character of this equation is obtained in agreement with the initial equation, i.e. it does not include the velocities. The influence of different superheated steam and of different system pressures is expressed by surfaces, densities, and interface tensions while different orifice dimensions are taken into account by the diameter.

The following table is a list of characteristic values allowing to mark the transition point in bubble formation.

The frequencies calculated by equation (5) agree well with the measured frequencies. The slight deviation towards lower values can be explained by the departure from the spherical geometry. The deformed bubble

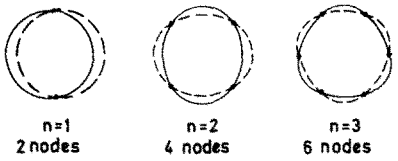

FIG. 10. Eigenoscillations of a sphere.

5. CONCLUSIONS

The formation of superheated steam bubbles is investigated at cylindrical single orifices while at the same time heat is transferred at high-system pressures and system temperatures. By evaluation of high-speed pictures statements can be made with respect to bubble volumes, interfaces, and frequencies of formation using the method of mechanics of similarity.

By variation of the mass flow through the orifice, the nozzle diameter, the system pressure, and the steam superheat the following results are obtained.

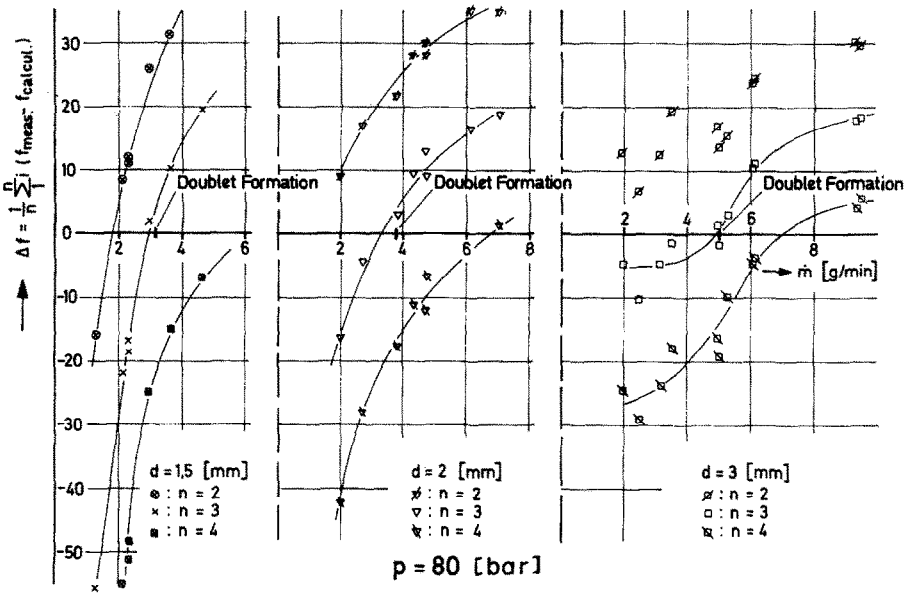

FIG. 11. Deviation between frequency of bubble formation and frequency of bubble eigenoscillation.

Table 1. Bubble frequencies in the transient zone of single bubble and twin bubble formation

d (mm)	p (at)	$\dot{m}$ (g/min)	O (mm^2)	$T_{ab}-T'$ /K/	f (s^{-1})	f_R (s^{-1})
1.5	40	1.85	52	60	55	59
	80	3.2	50.5	72	56	53
	120	4.0	45.5	58	60	51
2	40	2.5	85.5	44.3	46	43
	80	3.8	66	56	44	42
	120	4.0	48	53	45	42
3	40	4.5	155.6	63	30	27
	80	5	104	71	32	30
	120	5	56	64	37	36

surface effects that a too great spherical radius is put in the relation so that slightly lower frequencies are calculated. The same applies to Fig. 11 in which the calculated zero passage are found for slightly lower mass flows than in the observed transition of single bubble formation into twin bubble formation. The bubble deformation caused by detachment results in the calculation of slightly lower eigenfrequencies.

The calculated frequencies have been marked by an R in Fig. 6 and characterize the smallest frequencies of formation associated with the respective mass flow at the maximum bubble volume, that is the point where by mutual influencing of bubbles transition is observed from steady-state to unsteady-state bubble formation.

5.1 *Bubble volumes and interfaces*

In agreement with published experimental results obtained at atmospheric pressure the mass flow through the orifice as well as the orifice cross-section are of significant importance with respect to the size of the bubbles formed. It has been assumed so far that the transition from steady-state to turbulent aeration takes place in a narrow zone of mass flow. However, experiments performed show that non-steady-state bubble formation extends over a range of mass flow which is at least equal in size to that of steady-state aeration. Both ranges are constricted with a reduction in the orifice diameter and get extended with increasing system pressure. This tendency is observed up to system pressures near 120 at; at system pressures of about 160 at the range of bubble formation at the orifices occurs at slightly lower mass flows. Here, the adaption of physical properties between liquid and gas phase of water (ρ, η) and the interface (σ) becomes already effective. At a system pressure of 180 at the contours of the bubbles are very much influenced by the flow field: Distinct detachment events can no longer be observed but it occurs in an irregular succession of elongated

bubbles differing very much one from another in shape and size.

A further pressure increase to 212 at leads to a destruction of bubble contours and the phase boundaries are no longer clear-cut; a diffuse steam jet is observed.

In [13] bubble volumes of some 25 mm^3 are found for the steady-state range of formation for hydrogen and argon, respectively, in water at ambient temperature, using an orifice of 1.64 mm dia. and system pressures of 50 and 80 at. The measurements performed yield bubble volumes of roughly 30 mm^3 for the 1.5 mm dia. orifice in the steady-state range at a system pressure of 40 at and around 20 mm^3 at 80 at.

5.2 *Frequency of bubble formation*

In [13] abrupt increases in the frequency of formation are reported when the volume flow through the orifice is enhanced. These jumps in frequency are observed also in the experiments performed by the author of this paper. Besides indicating the laws underlying the frequency of bubble formation as a function of the dynamic parameters of the system, it is possible for the first time to take into account the modes of oscillation of the detaching bubbles as a variable which influences the mechanism of bubble formation. This is based on the Lamb formula of eigenoscillations for viscous spheroids. The area of the phase boundary of a bubble becomes a vibrational system under the impact of boundary surface tensions. The bubble is deformed by detachment and the resulting shape corresponds to its third eigenoscillation. If the bubble takes a size at which the related eigenfrequency of the third harmonic agrees with the frequency of bubble formation, the bubble is excited to make eigenoscillations. This causes such an abrupt detachment so that the formation of the consecutive bubble is prevented at the orifice and both bubbles coalesce.

REFERENCES

1. D. W. van Krevelen, Kinetic und Transporterscheingungen bei Reaktion in flüssig-gasförmigen Systemen, *Z. Elektrochem.* **57**(7), 502–512 (1953).
2. P. Grassman, Wärme- und Stoffaustausch zwischen zwei fluiden Phasen, *Chemie-Ingr-Tech.* **31**(3), 148–153 (1959).
3. T. Lohnstein, Zur Theorie des Abtropfens, *Ann. Phys.* **20**, 21, 22 (1906).
4. D. W. van Krevelen and P. J. Hoftijzer, Studies of gas-bubble formation: calculation of interfacial area in bubble contractors, *Chem. Engng Prog.* **46**(1), 29–35 (1950).
5. W, Siemes, Gasblasen in Flüssigkeiten, *Chemie-Ingr-Tech.* **26**(8/9), 479–496 (1954).
6. L. Davidson and E. H. Amick Jr., Formation of gas bubbles at horizontal orifices, *A.I.Ch.E. Jl* **2**(8), 337–342 (1956).
7. I. Leibson, E. G. Holcomb, A. G. Cacosa and J. J. Jacmic, Rate of flow and mechanics of bubble formation from single submerged orifices, *A.I.Ch.E. Jl* **2**(3), 296–306 (1956).
8. J. F. Davidson and B. O. G. Schüler, Bubble formation at an orifice in a viscous liquid, *Trans. Instn Chem. Engrs* **38**, 144–153 (1960).
9. R. R. Hughes, A. E. Handlos, H. D. Evans and R. L. Maycock, Thd formation of bubbles at single orifices, *Chem. Eng. Prog.* **51**(12), 557–563 (1955).
10. J. Zierep, *Ähnlichkeitsgesetze und Modellregeln der Strömungslehre.* G. Braun, Karlsruhe (1972).
11. H. Lamb, On the oscillations of a viscous spheroid, *Math. Soc. Proc. Lond.* **13**, 51–66 (1881).
12. H. Lamb, *Hydrodynamics.* Cambridge University Press, Cambridge (1932).
13. G. Kling, Über die Dynamik der Blasenbildung biem Begasen von Flüssigkeiten unter Druck, *Int. J. Heat Mass Transfer* **5**, 211–223 (1962).

FORMATION DES BULLES ET TRANSFERT THERMIQUE PENDANT LA DISPERSION DE LA VAPEUR SURCHAUFFEE DANS L'EAU SATURANTE. 1ERE PARTIE: DIMENSION DE LA BULLE ET DETACHEMENT DE LA BULLE A UN ORIFICE UNIQUE

Résumé—Malgré la grande importance pratique du transfert de chaleur et de masse entre les phases fluides, les données utilisables ne sont pas précises à cause de la multitude des paramètres qui interviennent dans ce phénomène. L'article contribue à ce vaste problème en se limitant au cas de la formation de la bulle à des orifices isolés. On considère expérimentalement la formation de la bulle et le départ d'orifices submergés à hautes pressions et températures. Dans la seconde partie est étudiée le transfert thermique associé. Les expériences sont conduites sur le système constitué par l'eau et sa vapeur. La vapeur surchauffée injectée par des orifices ayant des diamètres de 1,5, 2 et 3 mm et ouvert sur une chambre de 5 cm^3, débouche dans l'eau saturante et déminéralisée. Le débit de vapeur varie de 0,066–0,66 g/s, la pression étant égale à 212 bar. Les températures de la vapeur au dessus des températures d'ébullition correspondantes sont 100, 150 et 200 K. Les observations expérimentales sont liées par l'analyse dimensionnelle. On obtient les résultats suivants: des relations sont dégagées entre la forme des bulles la fréquence de formation et les paramètres physiques du système. On trouve que la transition entre la formation quasi-statique de la bulle (formation de la bulle unique) et la formation instationnaire (coalescence de bulles pendant le départ) est un problème d'oscillation propre de la bulle.

BLASENBILDUNG UND WÄRMEÜBERTRAGUNG BEIM EINBRINGEN VON HEISSDAMPF IN WASSER VON SÄTTIGUNGSTEMPERATUR—I. BLASENGRÖSSE UND ABLÖSEVORGÄNGE AN EINZELDÜSEN

Zusammenfassung—Die Angabe der Wärme- und Stoffübertragung zwischen fluiden Phasen ist trotz grosser praktischer Bedeutung wegen der Veilzahl beeinflussender Parameter lückenhaft. Die Arbeit behandelt ein Teilproblem dieses umfassended Themas, indem sie sich auf die Vorgänge bei der Blasenbildung an Einzeldüsen konzentriert.

Im vorliegenden 1. Teil der experimentellen Arbeit wird über Blasenbildung und Blasenablösung an Einzeldüsen bei hohen Systemdrücken und Temperaturen berichtet. Im Teil 2 wird die gleichzeitig ablaufende Wärmeübertragung untersucht.

Die Experimente werden im Einstoffsystem Dampf–Wasser durchgeführt. Überhitzter Wasserdampf strömt aus einem Dampfraum von 5 cm^3 Inhalt durch Düsen mit 1,5; 2 und 3 mm Durchmesser in vollentsalztes Wasser, das sich auf Sättigungstemperatur befindet. Der Heissdampfmassenstrom durch die Düse wird in einen Bereich von 2–20 g/min variiert, der maximale Systemdruck beträgt 212 at. Die Dampfüberhitzung, bezogen auf die jeweilige Siedetemperatur, erfolgt in drei Stufen: 100, 150 und 200 K.

Bei Variation von Systemdruck, Massenstrom durch die Düse, Düsendurchmesser und Dampfüberhitzung werden aufbauend auf den Aussagen der Dimensionsanalyse folgende Ergebnisse gewonnen: (i) Es werden Gesetzmässigkeiten zwischen der Blasengrösse sowie der Bildungsfrequenz und den Parametern des Systems angegeben. (ii) Die massgebende Ursache für den Umschlag von der stationären Blasenbildung (Einzelblasen-Bildung) in die instationäre Blasenbildung (Blasenvereinigung in Düsennähe) wird als ein Eigenschwingungsproblem erkannt und formelmässig erfasst.

ОБРАЗОВАНИЕ ПУЗЫРЬКОВ И ПРОЦЕСС ПЕРЕНОСА ТЕПЛА ПРИ ДИСПЕРСИИ ПЕРЕГРЕТОГО ПАРА В НАСЫЩЕННОЙ ВОДЕ. ЧАСТЬ 1. ДИАМЕТР И ОТРЫВ ПУЗЫРЬКОВ У ЕДИНИЧНЫХ ОТВЕРСТИЙ.

Аннотация — Несмотря на большое практическое значение тепло- и массообмена в двухфазной среде, этот вопрос еще недостаточно хорошо изучен из-за большого числа параметров, влияющих на данный процесс. В настоящей статье рассматривается часть этой обширной проблемы, а именно процессы, происходящие при образовании пузырьков у единичных отверстий. Целью работы является экспериментальное исследование зарождения и отрыва пузырьков у единичных затопленных отверстий при высоких давлениях и температурах в системе. Во второй части работы исследуется процесс теплообмена. Опыты проводились в системе пар-вода. Перегретый пар подавался через отверстия диаметром 1,5; 2 и 3 мм из камеры объёмом 5 $см^3$ в насыщенную обессоленную воду. Расход потока пара изменялся в диапазоне от 2 до 20 г/мин, давление составляло 212 атм. Обработка экспериментальных данных проводилась с помощью анализа размерностей. Выведены соотношения между формой пузырьков, а также частотой их образования и физическими параметрами системы. Найдено, что переход от стационарного зарождения пузырьков (образование единичных пузырьков) к нестационарному их образованию (слияние пузырьков при отрыве) зависит от собственных колебаний пузырьков.